minerals

MDPI

Article

Surface Organic Modification of $CaCO_3$-TiO_2 Composite Pigment

Sijia Sun, Hao Ding *, Yanpeng Zha, Wanting Chen and Zhuoqun Xu

Beijing Key Laboratory of Materials Utilization of Nonmetallic Minerals and Solid Wastes, National Laboratory of Mineral Materials, School of Materials Science and Technology, China University of Geosciences, Beijing 100083, China; ssjcugb@163.com (S.S.); zyp31012@sohu.com (Y.Z.); wantingchen123@163.com (W.C.); 2103170005@cugb.edu.cn (Z.X.)

* Correspondence: dinghao113@126.com

Received: 2 December 2018; Accepted: 11 February 2019; Published: 15 February 2019

Abstract: To improve the properties and dispersibility of $CaCO_3$-TiO_2 composite pigments ($CaCO_3$-TiO_2) in organic matrices, the surface modification of $CaCO_3$-TiO_2 was performed with sodium stearate (SS) as an organic modifier by wet ultra-fine grinding in a stirred mill. The pigment properties of modified $CaCO_3$-TiO_2 and its dispersibility in organic media were tested and characterized. The binding mechanism between $CaCO_3$-TiO_2 and SS was explored by infrared spectrometry (IR) and X-ray photoelectron energy spectroscopy (XPS). The results showed that the mechanical grinding strength and SS dosage had a significant effect on the activation index and sedimentation rate of $CaCO_3$-TiO_2. After surface modification, the surface of $CaCO_3$-TiO_2 turned from a hydrophilic surface to a hydrophobic surface and the surface free energy was reduced. In addition, the hiding property and dispersibility of $CaCO_3$-TiO_2 in the organic medium were significantly improved. IR and XPS results indicated that the modifier SS was adsorbed on the surface of $CaCO_3$-TiO_2 by chemical combination.

Keywords: $CaCO_3$-TiO_2 composite pigment; surface organic modification; dispersibility; modification mechanism

1. Introduction

Calcium carbonate ($CaCO_3$) is an important non-metallic mineral and $CaCO_3$ powder prepared by grinding natural mineral (such as calcite) and chemical precipitation has become the most commonly used filler added in various industrial products, such as plastics, coatings, and paper [1,2]. The preparation of composite pigments by uniformly coating TiO_2 on the surface of $CaCO_3$ particles is an important and efficient utilization of $CaCO_3$ mineral resources. Therefore, the related preparation processes have attracted wide attention [3,4]. Meanwhile, the preparation of the composite pigments can improve the utilization rate of pigment TiO_2 and reduce the consumption of expensive TiO_2 [5,6].

The TiO_2-coated $CaCO_3$ composite pigments can be prepared by several methods, such as mechanochemistry, carbonization reaction in a TiO_2 system, sol-gel, and hydrophobic aggregation methods, and the prepared $CaCO_3$-TiO_2 all exhibit the equivalent hiding power, oil absorption, and whiteness to the pigment TiO_2 [7,8]. However, the $CaCO_3$-TiO_2 prepared from the above methods except the hydrophobic agglomeration method have hydrophilic surface properties. Therefore, prepared $CaCO_3$-TiO_2 as a filler shows a poor dispersibility in organic products and its pigment function is largely affected [9,10]. Although the surface of $CaCO_3$-TiO_2 particles prepared by the hydrophobic aggregation method is hydrophobic, hydrophobic groups on the particle surface are often formed based on the combination of $CaCO_3$ and TiO_2 and the prepared composite pigment is not very compatible with the target application system. Moreover, industrially available

$CaCO_3$-TiO_2 produced by the mechanochemical method exhibits surface hydrophilicity. Therefore, it is necessary to conduct an organic modification of $CaCO_3$-TiO_2. In this way, $CaCO_3$-TiO_2 can obtain a hydrophobic surface, thus improving the compatibility of the composite pigments with organic systems, the functions of $CaCO_3$-TiO_2, and the performance of the final products.

Conventional surface modification technologies, such as the heating mixing modification and physical coating modification, have been applied in the treatment of fillers and pigments [11–13]. However, the $CaCO_3$-TiO_2 modified by the above two methods have some defects, such as an uneven dispersion between the modifier and materials and the absence of a reaction driving force caused by the weak stirring strength and low material mixing degree. Moreover, the hydrophobic modification effect is poor and the obtained products are unstable. Therefore, it is necessary to develop an efficient modification method.

Mechano-activated surface modification is a modification method utilizing the mechanochemical effect during the ultrafine grinding process. The method is thought to be more valuable and effective because the mechanochemical effect resulted from ultra-fine grinding can increase the activity of the mineral surface and enhance the reactivity in their interface [14,15]. The efficient method had been proved by the modification of some powder, such as $CaCO_3$ and wollastonite [16,17]. In this study, the surface organic modification of $CaCO_3$-TiO_2 with SS as the modifier by the wet mechanochemical method was investigated, and the pigment properties of modified $CaCO_3$-TiO_2 and its dispersibility in organic media were tested and characterized. Moreover, based on infrared spectrometry (IR) and X-ray photoelectron energy spectroscopy (XPS), the binding mechanism between $CaCO_3$-TiO_2 and SS was also explored.

2. Methods

2.1. Raw Materials

$CaCO_3$-TiO_2 was prepared by the mechanochemical method [18]. In as prepared $CaCO_3$-TiO_2, TiO_2 (50%, *w*/*w*) was uniformly coated on the surface of $CaCO_3$ and its main physical performance indicators are listed in Table 1.

Table 1. Physical performance indicators of $CaCO_3$-TiO_2 pigment.

Performance Indicators	Content of ~2 μm Fraction %	Whiteness %	Density (g/m^3)	Oil Absorption (g/100 g)	Hiding Power (g/m^2)	pH Value of Suspension
	92.5	94.5	3.1	21.9	19.6	6.8–9.5

The modifier sodium stearate (RCOONa, R stands for $C_{17}H_{35}$) is a chemically pure reagent (Beijing Chemical Plant, Beijing, China) with a white solid powder appearance. It was mixed with warm water to form a 5% (*w*/*v*) solution before use. Kerosene, *n*-hexane, and ethanol are all chemically pure reagents. Deionized water was used in the experiment.

2.2. Modification Method

Firstly, 50 g $CaCO_3$-TiO_2 was stirred with 200 g deionized water to form a slurry, which was ground together with an added 200 g grinding balls at 1000 rpm for 20 min. Three grinding balls with different diameters of 1.5 mm, 1.2 mm, and 0.8 mm were added according to the mass ratio of 1:1:1 in a GSDM-003 ultra-fine grinding mill (volume = 1 L). Secondly, SS solution was added into the $CaCO_3$-TiO_2 slurry according to the different mass ratios of SS to $CaCO_3$-TiO_2 powder (0%, 0.5%, 1%, 1.5%, 2%, and 3%) and the slurry was heated to different temperatures (20 °C, 50 °C, 80 °C, and 100 °C). Then, the slurry was ground to obtain the modified $CaCO_3$-TiO_2 slurry. Thirdly, the modified $CaCO_3$-TiO_2 slurry was separated from the grinding balls, dried, and then dispersed to obtain the modified $CaCO_3$-TiO_2.

2.3. Property Test of Modified $CaCO_3$-TiO_2

The organic modification degree of $CaCO_3$-TiO_2 was evaluated based on the sedimentation rate in kerosene (organic liquid medium) and the activation index of $CaCO_3$-TiO_2.

The sedimentation rate of the powder in the liquid medium was measured with a self-assembled measurement device (Figure 1). During the test, the weight of the powder on the sedimentation disk at any time from the beginning to the end of the settlement was recorded and then the mass percentage of the sedimentation powder to the total powder in the sedimentation zone was calculated as the sedimentation rate. The low sedimentation rate of particles in kerosene indicates the poor agglomeration effect, good dispersion effect, and the good hydrophobic surface caused by surface modification of the particles with SS [19].

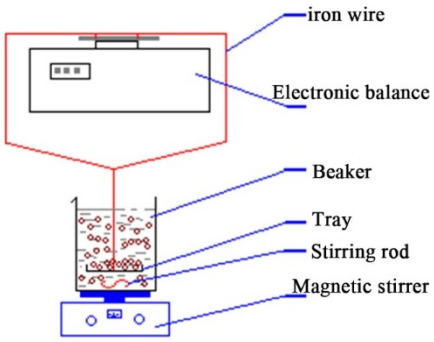

Figure 1. Measurement device of the sedimentation rate of powder samples.

The activation index refers to the mass proportion of the powder floating on water after powder is stirred in water [20]. Compared with particles with a hydrophilic surface, fine particles with a hydrophobic surface showed the increased adhesion of the three-phase wetted periphery at the water—vapor interface and could float at the interface because the adhesive force could be decomposed into the upward direction component. The larger activation index indicates the stronger adhesion and the better hydrophobic modification effect of particles. The test method of the activation index is described as follows. The modified powder was dispersed in water and stirred for 20 min. Then, after standing for several minutes, the weight of the powder floating on the water–gas interface was measured. Finally, the activation index was calculated as the mass ratio of the floating powder to the added powder.

To evaluate the surface wettability of THE modified $CaCO_3$-TiO_2 and provide the basis for the calculation of their surface free energy, the contact angle between $CaCO_3$-TiO_2 and the liquid medium was measured by a contact angle meter (JC2000D, Shanghai Zhongchen Digital Technic Apparatus Co., Ltd., Shanghai, China). The powder samples for the contact angle tests were processed by a tablet machine for measurement and the average of three measurements was adopted as the final result. Besides, the images of the $CaCO_3$-TiO_2 particles dispersed in different organic solvents were obtained by an image analyser (BT-1600, Bettersize Instruments Ltd., Dandong, China). The maximum resolution of the instrument was 0.1 μm and the images are the direct outputs of the instrument without processing.

The binding property between the modifier and $CaCO_3$-TiO_2 was explored by the analysis of Fourier transform infrared spectrum (FT-IR) and X-ray photoelectron spectroscope (XPS). The FT-IR spectra were recorded on an infrared spectrometer (Spectrum 100, PerkinElmer Instruments Co., Ltd., Waltham, MA, USA) in a scanning range of 400–4000 cm^{-1}. All samples were mixed with potassium bromide (KBr) according to a proportion of 1:100 to obtain the measurement slice. XPS measurements were carried out on an Escalab 250xi instrument (Thermo Fisher Scientific, Waltham, MA, USA) with monochromatic Al Kα X-ray radiation and the XPS lines were calibrated with the Cls line at 284.6 eV. The morphology of unmodified $CaCO_3$-TiO_2 and modified $CaCO_3$-TiO_2 composite particles was observed by scanning electron microscope (SEM, S-3500N, HITACHI, Tokyo, Japan). The particles' size

and specific surface area of $CaCO_3$-TiO_2 composite particles were tested by a centrifugal sedimentation particle size analyzer (BT-1500, Bettersize Instruments Ltd., Dandong, China).

The pigment properties of unmodified $CaCO_3$-TiO_2 and modified $CaCO_3$-TiO_2 were evaluated based on the tested oil absorption, hiding power, and whiteness. Oil absorption refers to the minimum amount of varnish (linseed oil) required for completely wetting 100 g of pigment and can be tested according to China National Standard GB/T5211.15-2014 [21]. Hiding power refers to the minimum amount of pigment required for completely covering per unit of black and white checkerboard. The hiding power of a pigment can be tested according to the National Industry Standards HG/T3851-2006 (the test method of pigment hiding power) [22]. The whiteness was tested with a whiteness meter (SBDY-1, Shanghai Yuet Feng Instrument Co., Ltd., Shanghai, China).

3. Results and Discussion

3.1. Influences of Modification Conditions on the Activation Index and Sedimentation Rate of $CaCO_3$-TiO_2

3.1.1. Influences of Modification Temperature

The sedimentation rate in kerosene and the activation index of $CaCO_3$-TiO_2 modified at different temperatures were investigated (Figure 2). The other experimental conditions were set as follows: SS dosage of 2.0 wt % (the mass ratio of SS to $CaCO_3$-TiO_2), grinding speed of 800 rpm, and grinding time of 25 min. With the rise of the modification temperature, the activation index of the modified $CaCO_3$-TiO_2 first increased gradually, reaching the maximum value (about 90%) at 80 °C, and then decreased slightly (Figure 2). With the rise of the modification temperature, the sedimentation rate of the modified $CaCO_3$-TiO_2 in kerosene decreased firstly, then reached the minimum at 80 °C and then increased. Therefore, the optimum modification temperature was 80 °C. It might be interpreted as follows. The low modification temperature is not conducive to the dissolution of the modifier in water and the hydrolysis of $RCOO^-$ to RCOOOH, thus reducing the content of effective components of the modifier and leading to the poor modification effect. However, the solvents evaporate too fast at higher temperatures, thus leading to an increase in the solid content and viscosity of the slurry and affecting the full contact between the modifier and composite particles.

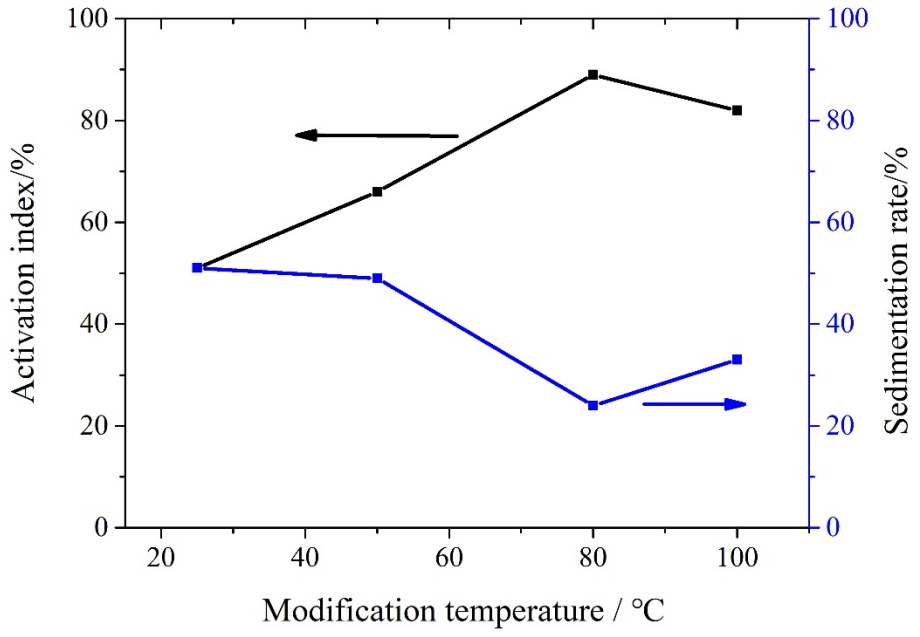

Figure 2. Influences of the modification temperature on the activation index and sedimentation rate of $CaCO_3$-TiO_2.

3.1.2. Influences of Modifier Dosage

Figure 3 shows the influences of the SS dosage on the activation index and sedimentation rate of $CaCO_3$-TiO_2. The modification temperature was 80 °C and the other experiment conditions were the same with those in Section 3.1.1. When the SS dosage increased from 0 to 2.0 wt %, the activation index of the modified products increased greatly, but the sedimentation rate decreased greatly (Figure 3). When the modifier dosage was more than 2.0 wt %, the activation index and sedimentation rate tended to be stable. The above results indicated that the minimum optimal dosage of SS was 2 wt %. It might be interpreted as follows. The modifier adsorbed on the surface of $CaCO_3$-TiO_2 had reached the saturation state under the dosage of 2 wt % and the excess modifier could not be adsorbed.

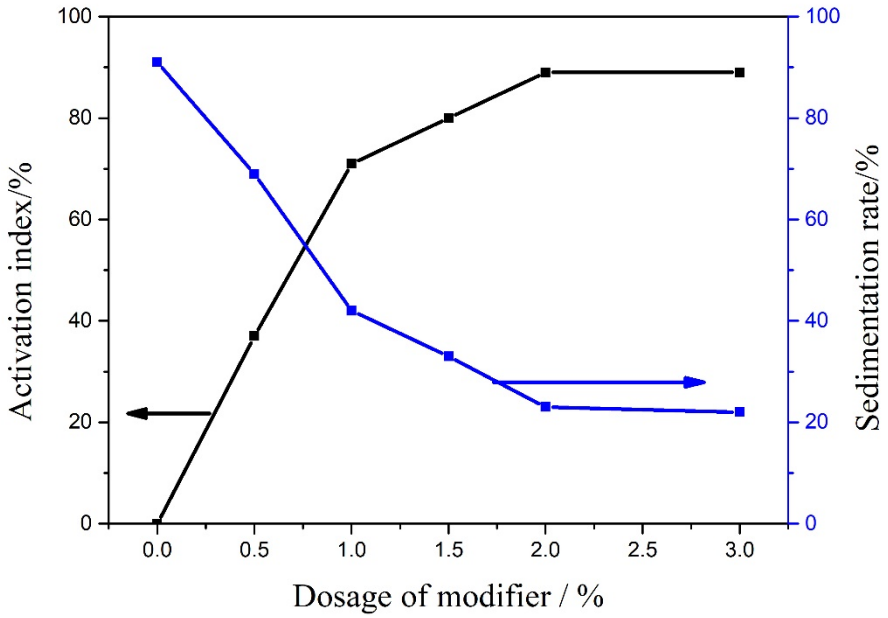

Figure 3. Influences of the modifier dosage on the activation index and sedimentation rate of $CaCO_3$-TiO_2.

3.1.3. Influences of the Mechanical Strength in Grinding

In the process of mechanical activation modification, the mechanical grinding force plays an important role in promoting the contact and bonding between the modifier and particle surface and the mechanical grinding strength is mainly determined by the grinding speed and grinding time. Therefore, the influences of the grinding speed and grinding time on the activation index and sedimentation rate of $CaCO_3$-TiO_2 were investigated (Figure 4). Under 2.0 wt % SS at 80 °C, the other experimental conditions were the same as those in Section 3.1.2. The grinding speed had little effect on the activation index and sedimentation rate of $CaCO_3$-TiO_2 (Figure 4a). In terms of the changes of the activation index and sedimentation rate, the modification effect increased with the increase of the grinding speed, but the increasing amplitude was not large. The optimum grinding speed was 1000 rpm. As the grinding time increased, the activation index of the modified $CaCO_3$-TiO_2 increased firstly and then decreased, whereas the sedimentation rate decreased firstly and then increased (Figure 4b). After 15-min of modification grinding, both the activation index and sedimentation rate indexes reached their optimal values. Obviously, the optimum modified grinding time was 15 min. It might be interpreted as follows. If the grinding time was too short, the mechanical strength was too low to activate the surface of $CaCO_3$-TiO_2, thus resulting in a weak reaction between $CaCO_3$-TiO_2 and SS ($RCOO^-$ or RCOOH). If the mechanical strength was too high, the modified products would be stripped and even the composite structure of $CaCO_3$-TiO_2 would be partly destroyed.

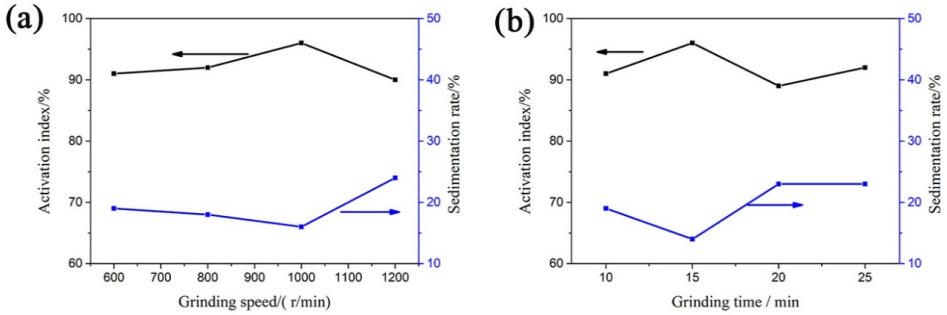

Figure 4. Influences of the grinding speed (**a**) and grinding time (**b**) on the activation index and sedimentation rate of $CaCO_3$-TiO_2.

3.2. Properties of Modified $CaCO_3$-TiO_2

3.2.1. Pigment Properties of Modified $CaCO_3$-TiO_2

The changes in the main pigment properties of $CaCO_3$-TiO_2 before and after modification are presented in Table 2. After wet mechanochemical modification, the hiding power of $CaCO_3$-TiO_2 decreased from 19.6 g/m^2 to 16.9 g/m^2 under 1.5 wt % SS and 16.7 g/m^2 under 2 wt % SS, indicating that the hiding property of $CaCO_3$-TiO_2 was improved significantly by wet mechanochemical modification. The oil absorption of $CaCO_3$-TiO_2 decreased significantly and the whiteness remained unchanged. Obviously, the surface organic modification by the mechanochemical method significantly improved the pigment performance of $CaCO_3$-TiO_2. According to the analysis of the pigment properties, the improvement in the hiding property of $CaCO_3$-TiO_2 by modification was mainly caused by the improvement in particle dispersion.

Table 2. Pigment properties of unmodified $CaCO_3$-TiO_2 and modified $CaCO_3$-TiO_2.

Samples	Oil Absorption (g/100 g)	Hiding Power (g/m^2)	Whiteness (%)
Unmodified $CaCO_3$-TiO_2	21.9	19.6	94.5
Modified $CaCO_3$-TiO_2-1.5%	16.4	16.9	94.2
Modified $CaCO_3$-TiO_2-2%	16.3	16.7	92.5

Note: X% in the modified $CaCO_3$-TiO_2-X% represents the dosage of SS.

3.2.2. Dispersion Properties

Figure 5 shows the images of unmodified $CaCO_3$-TiO_2 and modified $CaCO_3$-TiO_2 dispersed in ethanol (organic polar solvent) and kerosene (organic non-polar solvent). Unmodified $CaCO_3$-TiO_2 existed in the form of large-scale aggregates in ethanol and kerosene and the distribution of $CaCO_3$-TiO_2 was uneven (Figure 5a,b). The sizes of the aggregates in ethanol and kerosene were, respectively, larger than 100 μm and 200 μm, indicating the poor dispersion effect. As for the modified $CaCO_3$-TiO_2, although there were still some aggregates in ethanol and kerosene, the size of the aggregates significantly decreased below 10 μm (Figure 5c,d). The distribution of particles was more uniform, indicating that the dispersion of modified $CaCO_3$-TiO_2 in organic media was significantly improved. Undoubtedly, modification is an important factor for the improvement in the performance of $CaCO_3$-TiO_2. The result is consistent with Table 2.

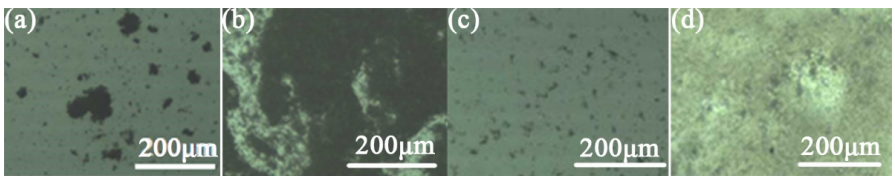

Figure 5. Images of unmodified $CaCO_3$-TiO_2 in ethanol (**a**) and kerosene (**b**) and modified $CaCO_3$-TiO_2 dispersed in ethanol (**c**) and kerosene (**d**).

3.2.3. Particle Characteristics

Figure 6 shows the scanning electron microscope (SEM) images of unmodified and modified $CaCO_3$-TiO_2. The unmodified and modified $CaCO_3$-TiO_2 samples exhibited a good coating morphology. Fine TiO_2 particles were uniformly and compactly coated on the surface of $CaCO_3$ particles, indicating that organic modification did not significantly change the structure and morphology of composite particles. Additionally, d_{50} and d_{90} of unmodified $CaCO_3$-TiO_2 were, respectively, 0.78 μm and 1.72 μm, and the d_{50} and d_{90} of modified $CaCO_3$-TiO_2 were, respectively, 0.72 μm and 1.65 μm. The specific surface areas of unmodified and modified $CaCO_3$-TiO_2 were, respectively, 6.29 g/m^2 and 6.41 g/m^2. Short-time grinding in the modification process did not cause a significant decrease in the particle size or a significant increase in the specific surface area of the composite particles, indicating that the composite particles were not significantly pulverized.

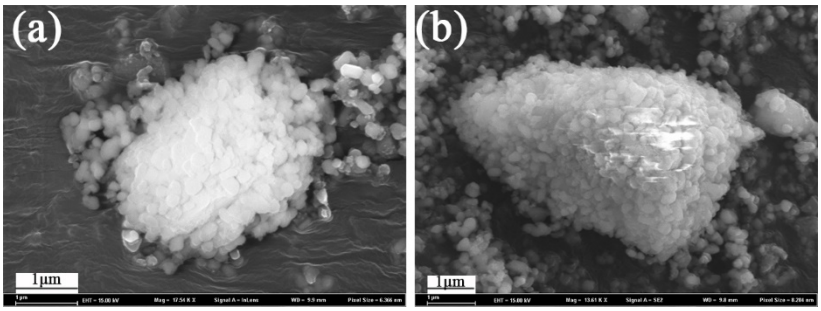

Figure 6. SEM images of (**a**) unmodified $CaCO_3$-TiO_2 and (**b**) modified $CaCO_3$-TiO_2.

3.3. Change in Surface Free Energy of $CaCO_3$-TiO_2 after Modification

3.3.1. Wetting Contact Angle of $CaCO_3$-TiO_2

The wetting contact angles of unmodified $CaCO_3$-TiO_2 and modified $CaCO_3$-TiO_2 (SS dosage = 0.5% and 1.5%) with distilled water, glycerol, and n-hexane are presented in Table 3. The contact angles of modified $CaCO_3$-TiO_2 with water and glycerol were greatly increased compared with that of unmodified $CaCO_3$-TiO_2 and the angles were further increased proportionally with the increase in SS dosage. However, the contact angle of modified $CaCO_3$-TiO_2 with *n*-hexane decreased, indicating that the organic modification of $CaCO_3$-TiO_2 resulted in a much weaker degree of wetting and the weaker interaction between $CaCO_3$-TiO_2 and the organic solvents (water and glycerol), whereas the interaction between $CaCO_3$-TiO_2 and *n*-hexane was enhanced. It could be inferred that the modification converted the polar surface of $CaCO_3$-TiO_2 into an organic non-polar surface, which was similar to *n*-hexane. Obviously, the conversion was ascribed to the adsorption of SS on the surface of $CaCO_3$-TiO_2.

Table 3. Wetting contact angle of $CaCO_3$-TiO_2 in different liquid media (°).

Samples	Water	Glycerol	Hexane
Unmodified $CaCO_3$-TiO_2	1.4	15.6	81.5
Modified $CaCO_3$-TiO_2-0.5%	70.5	73.0	75.0
Modified $CaCO_3$-TiO_2-1.5%	114.9	104.6	56.7

Note: X% in the modified $CaCO_3$-TiO_2-X% represents the dosage of SS.

3.3.2. Calculation of Surface Free Energy

When the solid particle is wetted by liquid, the relationship among the surface free energy of the solid, the surface free energy of the liquid, and the contact angle can be expressed as [23–25]:

$$(1 + \cos\theta)\gamma_L = 2[(\gamma_S{}^{LW}\gamma_L{}^{LW})^{1/2} + (\gamma_S{}^{+}\gamma_L{}^{-})^{1/2} + (\gamma_S{}^{-}\gamma_L{}^{+})^{1/2}] \quad (1)$$

where θ represents the wetting contact angle for the solid–liquid interface; γ_L and γ_S respectively represent the surface free energy of the liquid and solid; γ_L^+ and γ_L^- are, respectively, the electron acceptor part and the electron donor part in the polar component of γ_L; γ_S^+ and γ_S^- are, respectively, the electron acceptor part and the electron donor part in the polar component of γ_S; γ_L^{LW} and γ_S^{LW} are, respectively, the non-polar components of γ_L and γ_S.

The polarity component of γ_S^{AB} of γ_S can be calculated from γ_S^+ and γ_S^-:

$$\gamma_S^{AB} = 2(\gamma_S^+\gamma_S^-)^{1/2} \quad (2)$$

The γ_S can be calculated from γ_S^{AB} and γ_S^{LW}:

$$\gamma_S = \gamma_S^{LW} + \gamma_S^{AB} \quad (3)$$

The surface free energy parameters (γ_L, γ_L^{LW}, γ_L^+, and γ_L^-) of water, glycerol, and *n*-hexane are presented in Table 4 [26]. The values of γ_S and its components can be obtained by substituting the parameters in Table 4 and the wetting contact angle in Table 3 into Equation (1) based on Equations (2) and (3). The calculation results are shown in Table 5.

Table 5 shows that the surface free energy of $CaCO_3$-TiO_2 is greatly reduced after modification by SS and the decrease in amplitude is increased with the increase in SS dosage. When the dosage of SS was 1.5%, the γ_S value decreased from 74.21 mJ/m^2 to 11.62 mJ/m^2, and the decrease was as high as 62.59 mJ/m^2. From the perspective of the composition of γ_S, the decrease in the γ_S of $CaCO_3$-TiO_2 was mainly caused by the decrease of the polar component (γ_S^{AB}), whereas the non-polar component, γ_L^{LW}, was slightly improved. Due to the modification, the properties of the polar components on the particle surface were masked, whereas the non-polar properties of the alkyl chain of modifier were displayed. Since the change in the surface free energy of the particles was an important factor affecting the interface free energy and dispersion behavior of particles in the medium, it was considered that the above result was consistent with the change in the pigment performance of $CaCO_3$-TiO_2 (Table 2).

Table 4. Surface free energy parameters of different solvents (mJ/m^2).

Solvents	γ_L	γ_L^{LW}	γ_L^+	γ_L^-
Water	72.8	21.8	25.5	25.5
Glycerol	64.0	34.0	3.9	57.5
Hexane	18.4	18.4	0	0

Table 5. Surface free energy and its components of $CaCO_3$-TiO_2 (mJ/m^2).

Samples	γ_s	γ_s^{LW}	γ_s^{AB}	γ_s^+	γ_s^-
Unmodified $CaCO_3$-TiO_2	74.2	6.1	68.2	18.9	61.3
Modified $CaCO_3$-TiO_2-0.5%	28.1	7.3	20.8	4.2	25.7
Modified $CaCO_3$-TiO_2-1.5%	11.6	11.0	0.60	0.20	0.50

Note: X% in the modified $CaCO_3$-TiO_2-X represents the dosage of SS.

3.4. Binding Properties between $CaCO_3$-TiO_2 and Modifier

3.4.1. Infrared Spectral Analysis

To investigate the binding properties between the modifier and $CaCO_3$-TiO_2, the infrared spectra of unmodified $CaCO_3$-TiO_2, modified $CaCO_3$-TiO_2, and SS were analyzed (Figure 7). In the infrared spectra of $CaCO_3$-TiO_2, the absorption band at 3277 cm^{-1} is ascribed to the stretching vibration absorption band of hydroxyl groups, indicating that several hydroxyl groups or a small amount of coordination water molecules are adsorbed on the particle surface. The broadness of the peak indicates the existence of the association between hydroxyl groups. This is undoubtedly the consequence of the

dehydroxylation between $CaCO_3$ and TiO_2 and the hydration of TiO_2 in $CaCO_3$-TiO_2. The absorption bands at 1433 cm^{-1} and 874 cm^{-1} can be assigned to the asymmetric stretching vibration and bending vibration of CO_3^{2-} [27]. The broad band around 651 cm^{-1} is ascribed to the stretching vibrations of Ti–O bonds and the peak at 421 cm^{-1} is ascribed to the Ti–O–Ti bonds. In the infrared spectra of the modified $CaCO_3$-TiO_2, the characteristic absorption bands of –OH groups at 3414 cm^{-1} are different from those of $CaCO_3$-TiO_2 and the modifier SS due to the reaction between the hydroxyl groups of $CaCO_3$-TiO_2 and modifier SS. In addition to the characteristic bands of $CaCO_3$ and TiO_2, the observed characteristic band of SS at 2927 cm^{-1} is the characteristic peak of H–C–H asymmetric stretching vibrations. Therefore, it can be deduced that SS was adsorbed on the surface of $CaCO_3$-TiO_2. The characteristic peaks of COO^- at 1555 and 1443 cm^{-1} in the spectrum of SS might shift and coincide with the peak of CO_3^{2-} in the spectrum of modified $CaCO_3$-TiO_2 [28]. The above analysis indicates that the modifier is most likely to be chemisorbed on the surface of particles through the reaction of hydroxyl groups.

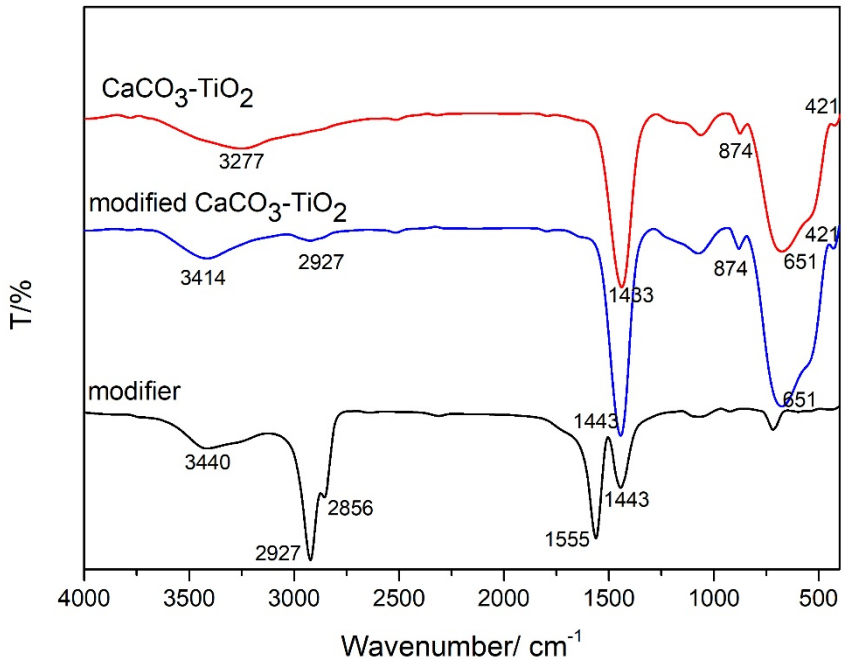

Figure 7. IR spectra of unmodified $CaCO_3$-TiO_2, modified $CaCO_3$-TiO_2, and modifier sodium stearate (SS).

3.4.2. XPS Analysis

Figure 8 shows the XPS spectra of unmodified $CaCO_3$-TiO_2 and modified $CaCO_3$-TiO_2 as well as the changes in the binding energy of Ca and Ti. In Figure 8a, the peaks appeared at 346.92 eV and 350.48 eV in the XPS spectrum of unmodified $CaCO_3$-TiO_2 and correspond to $Ca2p_{3/2}$ and $Ca2p_{1/2}$. It can be seen that there is no significant displacement of Ca in the binding energy after the modification of $CaCO_3$-TiO_2. In Figure 8b, the peaks at 458.41 eV and 464.10 eV in the XPS spectra of unmodified $CaCO_3$-TiO_2 correspond to $Ti2p_{3/2}$ and $Ti2p_{1/2}$ [29]. In the XPS spectrum of modified $CaCO_3$-TiO_2, the corresponding peaks of Ti2p at 458.35 eV and 464.04 eV show no obvious displacement compared with those of unmodified $CaCO_3$-TiO_2, indicating that the chemical environment of the Ti element is unchanged after modification. In other words, the modifier does not chemically bond with Ti^{4+} directly. Due to the strong hydration of TiO_2, the surface of TiO_2 is covered by a large number of hydroxyl groups [30], and the change in the outermost hydroxyl groups has little effect on the binding energy of Ti atoms. The results of the IR spectrum and XPS spectra indicate that $CaCO_3$-TiO_2 may bond with SS through the dehydroxylation between hydroxyl groups on the surface of TiO_2 and SS.

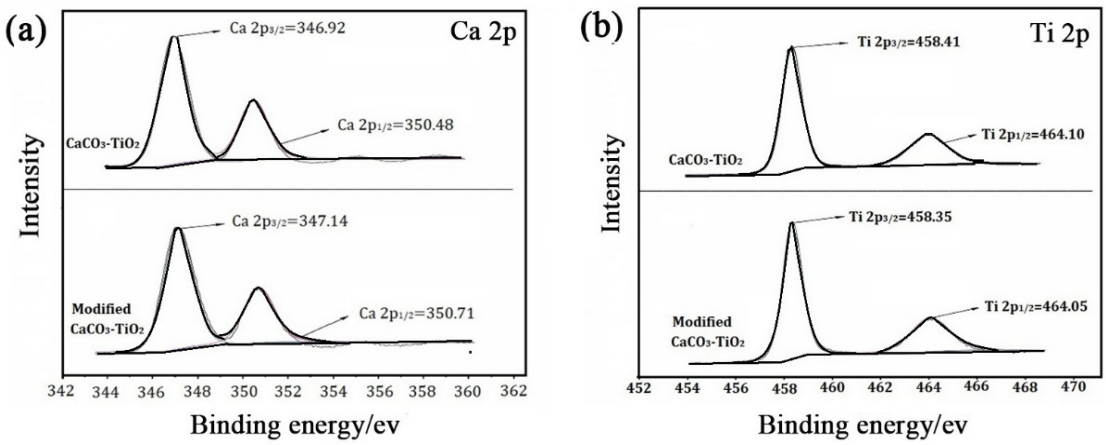

Figure 8. XPS spectra of unmodified and modified $CaCO_3$-TiO_2: Curve fitting analysis of (**a**) Ca 2p and (**b**) Ti 2p.

3.4.3. Surface Organic Modification Model of $CaCO_3$-TiO_2

According to the above analysis, SS was chemisorbed on the surface of $CaCO_3$-TiO_2 and this adsorption occurred mainly in the TiO_2 region on the surface of the composite particles.

There is a small number of uncovered $CaCO_3$ and a large number of coating TiO_2 on the surface of $CaCO_3$-TiO_2 [18]. For $CaCO_3$, its outermost surfaces are coated by TiO_2 and there are only a small number of unsaturated Ca^{2+} and CO_3^{2-} on its surface. In the aqueous medium, Ti^{4+} on the surface of TiO_2 is strongly hydrolyzed to form hydrolyzates (mainly including Ti^{4+} hydroxylate), which finally form a surface morphology of TiO_2 dominated by hydroxyl groups [31]. Therefore, the hydroxyl in TiO_2 is the group involved in the chemical reactions between TiO_2 and the modifier. The modifier SS will undergo the following hydrolysis reactions in aqueous medium:

$$RCOONa \rightarrow RCOO^- + Na^+, \quad (4)$$

$$RCOO^- + H_2O \rightleftarrows RCOOH + OH^- \quad (5)$$

Therefore, RCOOH should be the main group involved in the chemical reactions between the modifier and $CaCO_3$-TiO_2.

Based on the above analysis, the surface organic modification model of $CaCO_3$-TiO_2 by SS was established (Figure 9).

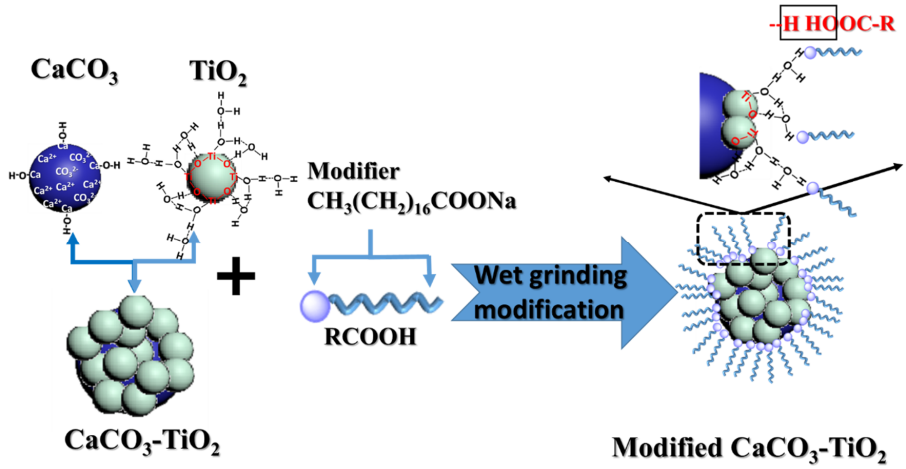

Figure 9. Surface organic modification model of $CaCO_3$-TiO_2 by SS.

4. Conclusions

(1) The surface organic modification of $CaCO_3$-TiO_2 was carried out by the wet mechanical grinding method with sodium stearate as the modifier. The modification temperature, dosage of modifier, and mechanical strength in grinding are the important factors of the activation index and sedimentation rate of $CaCO_3$-TiO_2. After modification, the hydrophilic surface of $CaCO_3$-TiO_2 was converted into a hydrophobic surface. The activation index of $CaCO_3$-TiO_2 in aqueous medium reached 97% and the water wetting contact angle reached 114.9° under 1.5 wt % SS. The dispersibility of modified $CaCO_3$-TiO_2 in ethanol and kerosene was significantly improved.

(2) The calculation results of the surface free energy showed that after the modification, the properties of polar components on the surface of $CaCO_3$-TiO_2 were masked, whereas the organic non-polar properties of SS were displayed, thus changing the dispersion behaviors of $CaCO_3$-TiO_2. When the dosage of SS was 1.5%, the γ_s value decreased from 74.2 mJ/m^2 to 11.6 mJ/m^2.

(3) Modification leads to a significant improvement in the pigment properties of $CaCO_3$-TiO_2. The hiding power of $CaCO_3$-TiO_2 dropped from 19.6 g/m^2 to 16.9 g/m^2 under 1.5 wt % SS and 16.7 g/m^2 under 2 wt % SS after modification.

(4) The modifier was chemisorbed on the surface of particles. The binding of the modifier with $CaCO_3$-TiO_2 was mainly induced by the dehydroxylation of RCOOH and hydroxyl groups on the TiO_2 surface.

Author Contributions: S.S., H.D., Y.Z., W.C. and Z.X. conceived and designed the experiments; S.S. and Y.Z. performed the experiments; S.S. and H.D. wrote the paper.

Funding: This work was supported by the National Natural Science Foundation of China (Grant No. 51474194).

Conflicts of Interest: The authors have declared that there are no competing interests existing in this research.

References

1. Zhang, Q.; Yu, Z.; Xie, X.; Mai, Y. Crystallization and impact energy of polypropylene/$CaCO_3$ nanocomposites with nonionic modifier. *Polymer* **2004**, *45*, 5985–5994. [CrossRef]
2. Hu, Z.; Zen, X.; Gong, J.; Deng, Y. Water resistance improvement of paper by superhydrophobic modification with microsized $CaCO_3$, and fatty acid coating. *Colloid Surf. A* **2009**, *351*, 65–70. [CrossRef]
3. Tao, H.; He, Y.; Zhao, X. Preparation and characterization of calcium carbonate–titanium dioxide core–shell ($CaCO_3$ @TiO_2) nanoparticles and application in the papermaking industry. *Powder Technol.* **2015**, *283*, 308–314. [CrossRef]
4. Zhang, L. Preparation of nanosized anatase TiO_2-coated kaolin composites and their pigmentary properties. *Powder Technol.* **2009**, *196*, 122–125.
5. Gao, Q.; Wu, X.; Xia, Z.; Fan, Y. Coating mechanism and near-infrared reflectance property of hollow fly ash bead/TiO_2 composite pigment. *Powder Technol.* **2017**, *305*, 433–439. [CrossRef]
6. Zhao, X.; Li, J.; Liu, Y.; Zhang, Y.; Qu, J.; Qi, T. Preparation and mechanism of TiO_2-coated illite composite pigments. *Dyes Pigments* **2014**, *108*, 84–92. [CrossRef]
7. Li, Z.; Huang, C.; Guo, L.; Cui, L.; Zhou, B. Mass production and application of TiO_2@$CaCO_3$ composites in interior emulsion coatings. *Colloid Surf. A* **2016**, *498*, 98–105. [CrossRef]
8. Sun, S.; Ding, H.; Hou, X.; Chen, D.; Yu, S.; Zhou, H.; Chen, Y. Effects of organic modifiers on the properties of TiO_2-coated $CaCO_3$ composite pigments prepared by the hydrophobic aggregation of particles. *Appl. Surf. Sci.* **2018**, *456*, 923–931. [CrossRef]
9. Morsy, F.; El-Sherbiny, S.; Hassan, M.; Mohammed, H. Modification and evaluation of Egyptian kaolinite as pigment for paper coating. *Powder Technol.* **2014**, *264*, 430–438. [CrossRef]
10. Zhou, H.; Sun, S.; Ding, H. Surface organic modification of TiO_2 powder and relevant Characterization. *Adv. Mater. Sci. Eng.* **2017**, *2017*, 9562612. [CrossRef]
11. Lin, J.; Siddiqui, J.A.; Ottenbrite, R.M. Surface modification of inorganic oxide particles with silane coupling agent and organic dyes. *Polym. Adv. Technol.* **2001**, *12*, 285–292. [CrossRef]

12. Bagwe, R.P.; Hilliard, L.R.; Tan, W. Surface Modification of silica nanoparticles to reduce aggregation and nonspecific binding. *Langmuir* **2006**, *22*, 4357–4362. [CrossRef]
13. Jiang, D.; Xu, Y.; Hou, B.; Wu, D.; Sun, Y. Synthesis of visible light-activated TiO_2 photocatalyst via surface organic modification. *J. Solid State Chem.* **2007**, *180*, 1787–1791. [CrossRef]
14. Palaniandy, S.; Azizli, K.A.M. Mechanochemical effects on talc during fine grinding process in a jet mill. *Int. J. Miner. Process.* **2009**, *92*, 22–33. [CrossRef]
15. Romeis, S.; Schmidt, J.; Peukert, W. Mechanochemical aspects in wet stirred media milling. *Int. J. Miner. Process.* **2016**, *156*, 24–31. [CrossRef]
16. Ding, H.; Lu, S.C.; Deng, Y.X.; Du, G.X. Mechano-activated surface modification of calcium carbonate in wet stirred mill and its properties. *Trans. Nonferrous Met. Soc.* **2007**, *17*, 1100–1104. [CrossRef]
17. Ding, H.; Lu, S.; Du, G. Surface modification of wollastonite by themechano-activated method and its properties. *Int. J. Miner. Metall. Mater.* **2011**, *18*, 83–88. [CrossRef]
18. Sun, S.; Ding, H.; Hou, X. Preparation of $CaCO_3$-TiO_2 composite particles and their pigment properties. *Materials* **2018**, *11*, 1131. [CrossRef]
19. Ding, H. *Surface Modification of Powder and Its Application*; Tsinghua University Press: Beijing, China, 2013.
20. Luo, Z.; Zhu, J.F.; Tang, L.G.; Zhao, Y.M.; Guo, J.; Zuo, W.; Chen, S.L. Fluidization characteristics of magnetite powder after hydrophobic surface modification. *Int. J. Miner. Process.* **2010**, *94*, 166–171. [CrossRef]
21. *GB/T5211.15-2014, General Methods of Test for Pigments and Extenders*; Standards Press of China: Beijing, China, 2014.
22. *HG/T3851-2006, Covering Power Determination of Dyestuff*; National Development and Reform Commission: Beijing, China, 2006.
23. Qiu, G.; Hu, Y.; Wang, D. *Interactions between Particles and Flotation of Fine Particles*; Central South University Press: Chnagsha, China, 1993.
24. Farahat, M.; Hirajima, T.; Sasaki, K. Adhesion of Ferroplasma acidiphilum onto pyrite calculated from the extended DLVO theory using the van Oss-Good-Chaudhury approach. *J. Colloid Interface Sci.* **2010**, *349*, 594–601. [CrossRef]
25. Fowkes, F.M. Determination of interfacial tensions, contact angles, and dispersion forces in surfaces by assuming additivity of intermolecular interactions in surfaces. *J. Phys. Chem.* **1962**, *66*, 382. [CrossRef]
26. Li, Z.; Giese, R.F.; Vanoss, C.J.; Yvon, J.; Cases, J. The surface thermodynamic properties of talc treated with octadecylamine. *J. Colloid Interface Sci.* **1993**, *156*, 279–284. [CrossRef]
27. Legodi, M.A.; Waal, D.D.; Potgieter, J.H.; Potgieter, S.S. Rapid determination of $CaCO_3$ in mixtures utilising FT-IR spectroscopy. *Miner. Eng.* **2001**, *14*, 1107–1111. [CrossRef]
28. Tran, H.V.; Tran, L.D.; Vu, H.D.; Thai, H. Facile surface modification of nanoprecipitated calcium carbonate by adsorption of sodium stearate in aqueous solution. *Colloid Surf. A* **2010**, *366*, 95–103. [CrossRef]
29. Akple, M.S.; Low, J.; Qin, Z.; Liu, S. Nitrogen-doped TiO_2 microsheets with enhanced visible light photocatalytic activity for CO_2 reduction. *Chin. J. Catal.* **2015**, *36*, 2127–2134. [CrossRef]
30. Bezrodna, T.; Puchkovska, G.; Shymanovska, V.; Baran, J.; Ratajczak, H. IR-analysis of H-bonded H_2O on the pure TiO_2 surface. *J. Mol. Struct.* **2004**, *700*, 175–181. [CrossRef]
31. Perrin, D.D. *Stability Constants of Metal-Ion-Complexes*; Pergamon Press: Oxford, UK, 1979.